

Journal Pre-proofs

New tranlycypromine derivatives containing sulfonamide motif as potent LSD1 inhibitors to target acute myeloid leukemia: design, synthesis and biological evaluation

Liyun Liang, Haiwen Wang, Yongliang Du, Bingling Luo, Ning Meng, Meifeng Cen, Peng Huang, A. Ganesan, Shijun Wen

PII: S0045-2068(20)30298-4
DOI: <https://doi.org/10.1016/j.bioorg.2020.103808>
Reference: YBIOO 103808

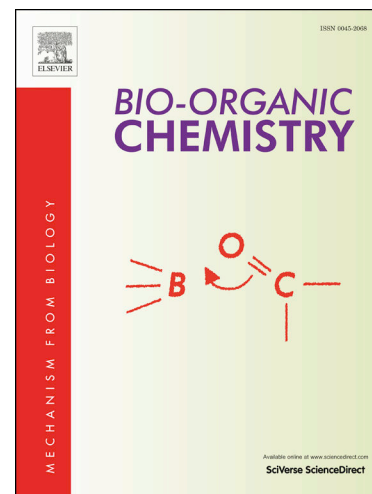
To appear in: *Bioorganic Chemistry*

Received Date: 6 February 2020
Revised Date: 20 March 2020
Accepted Date: 29 March 2020

Please cite this article as: L. Liang, H. Wang, Y. Du, B. Luo, N. Meng, M. Cen, P. Huang, A. Ganesan, S. Wen, New tranlycypromine derivatives containing sulfonamide motif as potent LSD1 inhibitors to target acute myeloid leukemia: design, synthesis and biological evaluation, *Bioorganic Chemistry* (2020), doi: <https://doi.org/10.1016/j.bioorg.2020.103808>

This is a PDF file of an article that has undergone enhancements after acceptance, such as the addition of a cover page and metadata, and formatting for readability, but it is not yet the definitive version of record. This version will undergo additional copyediting, typesetting and review before it is published in its final form, but we are providing this version to give early visibility of the article. Please note that, during the production process, errors may be discovered which could affect the content, and all legal disclaimers that apply to the journal pertain.

© 2020 Published by Elsevier Inc.



New tranlycypromine derivatives containing sulfonamide motif as potent LSD1 inhibitors to target acute myeloid leukemia: design, synthesis and biological evaluation

Liyun Liang ^a, Haiwen Wang ^a, Yongliang Du ^a, Bingling Luo ^a, Ning Meng ^a, Meifeng Cen ^b, Peng Huang ^a, A. Ganesan ^c, Shijun Wen ^{*,a}

^a State Key Laboratory of Oncology in South China, Collaborative Innovation Center for Cancer Medicine, Sun Yat-sen University Cancer Center, 651 Dongfeng East Road, Guangzhou 510060, China

^b Medical Research Center, Sun Yat-sen Memorial Hospital, Sun Yat-sen University, Guangzhou, Guangdong 510120, China

^c School of Pharmacy, University of East Anglia, Norwich Research Park, Norwich NR4 7TJ, United Kingdom

Abstract

Lysine-specific demethylase 1 (LSD1) is frequently elevated in acute myeloid leukemia (AML) and often leads to tumorigenesis. In recent years, numerous LSD1 inhibitors based on tranylcypromine (TCP) scaffolding have reached clinical trials. Most TCP derivatives were modified at the amino site of cyclopropane motif. Herein, we for the first time introduced a sulfonamide group in TCP benzene ring of series **a** compounds and performed a systematical study on structure and activity relationships by varying sulfonamide groups. The introduction of sulfonamide significantly increased the targeting capacity of TCP against LSD1. Moreover, we discovered that the Boc attached LSD1 inhibitors (labelled as series **b** compounds) substantially improved their anti-proliferation capacity towards AML cells. The intracellular thermal shift and LC-MS/MS results implied that Boc enhanced the drug lipophilicity and might be removed under the cancerous acidic environment to release the real pharmacophore, evidenced by the fact that a structurally similar but acidic inert pivaloyl to replace Boc dramatically dropped the cellular anti-proliferation effect. Finally, a benzyl group installed at the amino site to appropriately increase lipophilicity led to trans-4-(2-(benzylamino)-cyclopropyl)-*N,N*-diethylbenzenesulfonamide **a10** that showed better anti-proliferation activity in AML cells and enzymatic inhibition against LSD1. Taken together, our work offers a novel TCP-based structure and provides a prodrug strategy for the discovery of potent LSD1 inhibitors by having appropriate lipophilicity.

Keywords: Lysine-specific demethylase 1; Inhibitor; Acute myeloid leukemia; Lipophilicity; Prodrug.

1. Introduction

Aberrant epigenetic modification is a hallmark of hematological malignancy and correlated with the leukemic transformation.[1, 2] Simultaneously, epigenetic regulation is a highly dynamic process manipulated by multiple enzymes, and such process can be used as a potential drug target.[3-6] An epigenetic modification enzyme, lysine-specific demethylase 1 (LSD1, also known as KDM1A), is a nuclear amine oxidase homolog and specifically targets mono- and di-methylated lysine 4 and lysine 9 of histone H3 (H3K4me1/2, H3K9me1/2) using flavin adenine dinucleotide (FAD) as the coenzyme.[7-11] Evidences suggest that LSD1 is often elevated in acute myeloid leukemia (AML), particularly poor-differentiated AML harboring chromosomal translocation.[12] A combination of LSD1 inhibitors with all-trans-retinoic acid (ATRA) has been used to break the differentiation blockade in AML.[13] Therefore, LSD1 is emerging as an essential target for AML therapy.

In the past decades, numerous LSD1 inhibitors were developed and could be divided into irreversible and reversible types according to their action mechanisms.[14-25] Currently, irreversible LSD1 inhibitors based on tranylcypropane (TCP) scaffolding have achieved good progress, illustrated by the two most advanced drug candidates ORY-1001 and GSK2879552 (Figure 1A).[26, 27] Their inhibition mechanism involves the formation of an amine cation radical to covalently react with FAD to block the biological function of LSD1 (Figure 1B). As far as we know, ORY-1001 and GSK2879552 have entered into phase I clinical trials with enzymatic inhibition at a nanomolar level (Figure 1C). The development of irreversible LSD1 inhibitors often focuses on the alteration of the cyclopropane amino side, and there are relatively few reports of modifications on the benzene ring.[28-31] The sulfonamide group is frequently employed in the drug development [32] and it is shaped in a tetrahedron three-dimension, very different from the planar amides.[33] Thus, it was of our interest to install a sulfonamide on the benzene ring of TCP to develop novel potent LSD1 inhibitors.

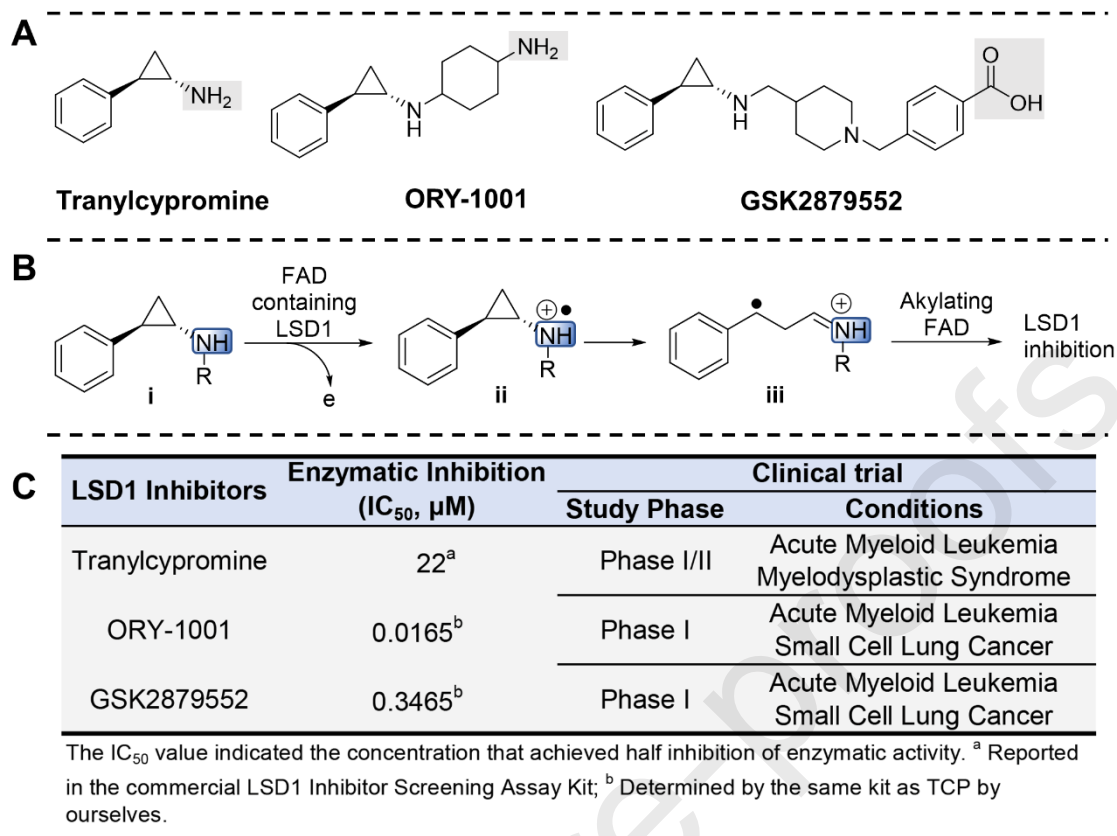


Figure 1. (A) The structures, (B) inhibitory mechanism and (C) enzymatic activities of three representative irreversible LSD1 inhibitors based on TCP scaffolding.

2. Results and discussion

2.1. Chemistry

Numerous LSD1 inhibitors were often modified at the cyclopropane amino side. Structure-activity relationship studies (SARs) on the benzene ring were relatively scant, for example, a reported LSD1 inhibitor T-3775440 has a para-positioned carboxamide.[34] For the first time, we introduced the sulfonamide group at the benzene ring side of TCP to develop novel LSD1 inhibitors (Figure 2). As a result, a series of compounds defined as series **a** was designed. Simultaneously, in our previous work, compounds with Boc group contributed to an increased cellular uptake, and it was of our interest to further explore its advantage. Thus, Boc group was newly introduced at the cyclopropane amino side to obtain series **b** compounds. Meanwhile, **c9** with a structurally similar pivaloyl was also designed.

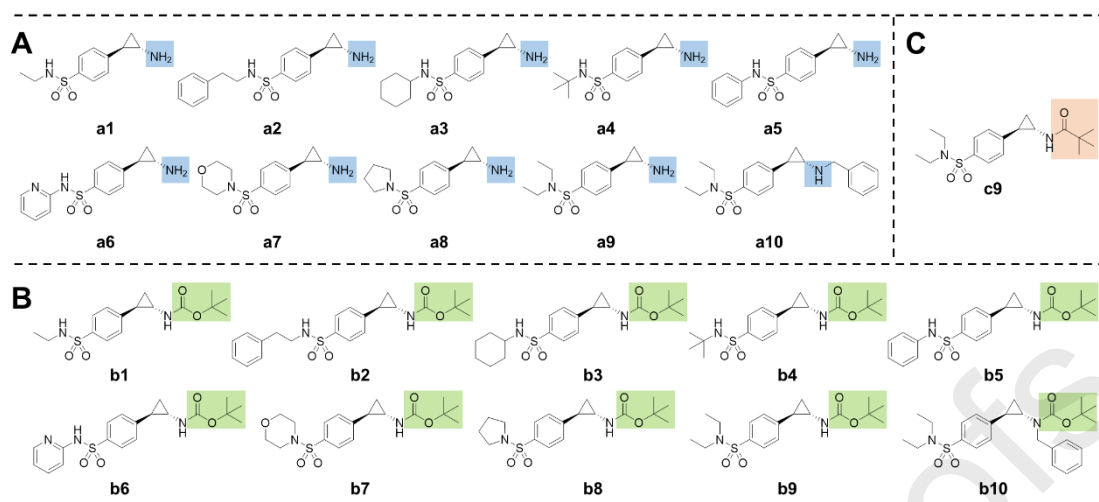
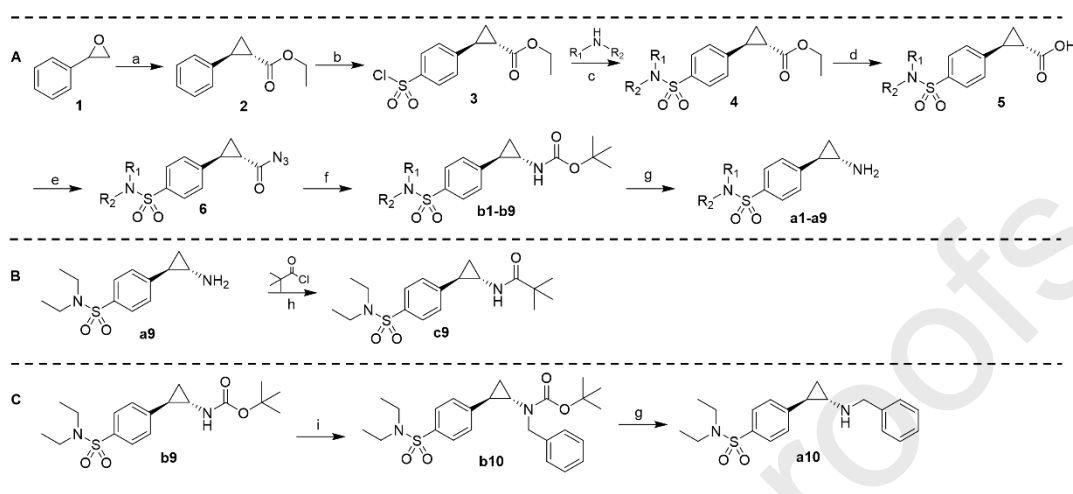


Figure 2. The racemic compounds designed from tranlycypromine. (A) Series **a** compounds with a free amine. (B) Series **b** compounds with Boc at the cyclopropane amino site. (C) Series **c** compound with a pivaloyl.

All the racemic compounds **a1-a10**, **b1-b10** and **c9** were synthesized via the routes described in Scheme 1. Commercially available 2-phenyloxirane (labeled as **1**) was reacted with triethyl phosphonoacetate in the presence of *n*-BuLi to acquire trans-cyclopropyl ester **2**.^[33] Following a procedure of Huntress' work,^[35] **2** was treated with chlorosulfonic acid in anhydrous dichloromethane, and a chlorosulfonyl group was successfully installed in the para position of the benzene ring to afford compound **3**. Then, a series of different amino groups were added respectively to get **4** with varying sulfonamides. Series **b** compounds **b1-b9** were then obtained after three steps. Firstly, **4** were hydrolyzed into acids **5** under subsection to LiOH, and the following coupling reaction with DPPA at room temperature provided acyl azide **6**. Curtius rearrangement in the refluxing *t*-BuOH resulted in the formation of compounds **b1-b9**. Meanwhile, deprotection of Boc using HCl in methanol gave series **a** compounds **a1-a9** in a hydrochloride salt form (Scheme 1A). For the preparation of **c9**, compound **a9** reacted with pivaloyl chloride in presence of DIPEA to assemble **c9** (Scheme 1B). Additionally, compound **b10** was also synthesized from **b9** by introducing a benzyl group (Scheme 1C), and the Boc deprotection from **b10** afforded compound **a10**. As a result, both alkyl and aryl primary amines as well as both cyclic and acyclic secondary amines were

installed to construct three series of novel sulfonamide TCP derivatives for further anticancer screening.



Scheme 1. Synthesis of the designed compounds. Reagents and conditions: (a) triethyl phosphonoacetate, *n*-BuLi, 1,4-dioxane, r.t., then microwave at 135 °C for 60 min; (b) chlorosulfonic acid, anhydrous CH₂Cl₂, 0 °C-r.t., 3 h; (c) DIPEA, anhydrous CH₂Cl₂, 0 °C-r.t., 2 h; (d) THF/H₂O (3:1), LiOH, r.t., 3 h; (e) Et₃N, DPPA, THF, r.t., 4 h; (f) *t*-BuOH, reflux, 12 h; (g) HCl/MeOH, r.t., 2 h; (h) DIPEA, anhydrous CH₂Cl₂, r.t., 2 h; (i) NaH, benzyl bromide, THF, r.t., 2 h. Note: the compounds are racemic.

2.2. Preliminary anti-proliferation screening of modified TCP derivatives at the cellular level

The selection of appropriate cancer cell lines to evaluate the anti-proliferation effect of inhibitors is essential for acquiring realistic results. Several reports have studied drug sensitivity to LSD1 inhibitors in numerous cell lines of hematopoietic malignancy, and acute myeloid leukemia MV4-11 was regarded as the drug-sensitive cell line towards LSD1 inhibition.[36, 37] Before the preliminary screening of our synthetic compounds, we wanted to confirm the reported results firstly. LSD1 was significantly elevated in acute myeloid leukemia via analyzing patient-derived data from the Oncomine database (Figure S1A). After ORY-1001 and GSK2879552 were confirmed to inhibit LSD1 at nanomolar concentrations (Figure 1C), these two compounds and TCP were employed to screen AML cell lines treated with each drug at 5 μM for 8 days. Among six tested

AML cell lines, MV4-11 was found to be most sensitive towards LSD1 inhibition, which was consistent with literature reports (Figure 3A and Figure S1B-F).[36] Although both ORY-1001 and GSK2879552 quickly reached 40 % inhibition of cancer cell growth at low concentrations ($< 1 \mu\text{M}$), they could not inhibit cell growth further at higher concentrations (Figure 3B). The results suggested that the development of more potent LSD1 inhibitors to increase their cellular anti-proliferation capacity would be highly favorable.

Compounds **a1-a9** and **b1-b9** were screened for their anti-proliferation capacity using MV4-11 cell line at three gradient concentrations ($1 \mu\text{M}$, $10 \mu\text{M}$ and $30 \mu\text{M}$) via MTS assay, as shown in Figure 3C-E. At a low concentration of $1 \mu\text{M}$, most of the synthetic compounds did not prevent cancerous cell growth obviously. While the dosage increased ($10 \mu\text{M}$ and $30 \mu\text{M}$), some compounds especially **b9** started to show substantial anti-proliferation capacity, which was significantly better than the three typical positive compounds (TCP, ORY-1001 and GSK2879552). Series **b** compounds with Boc group exhibited better anti-proliferation activity than the corresponding series **a** compounds with only free amines at $10 \mu\text{M}$ and $30 \mu\text{M}$ (Figure 3F).

Compared to the simple TCP, the lipophilic alkylsulfonamides seemingly increased the anti-proliferation potency of many of series **b** compounds. Notably, the best compound **b9** almost fully inhibited the cell growth of MV4-11, much better than three well-known LSD1 inhibitors. CLogP is a classic parameter representing lipid solubility, and its range between 1 to 5 is optimal for the drug development. To study the potential relationship between lipophilicity and anti-proliferation capacity of the synthetic compounds, CLogP values were calculated by ChemDraw and the correlation analysis was conducted through GraphPad Prism. Series **a** compounds exhibited a lower CLogP value (< 2.4), likely leading to the worse cellular uptake. Consequently, the cell growth inhibitory rate of **a1-a9** at $30 \mu\text{M}$ were below 50 % (Table S1). Introduction of Boc group improved the lipophilicity of compounds **b1-b9**, and the inhibition rates were elevated as a result. Especially, while the ClogP reached the range of between 3.0 and 4.0, the anti-proliferation capacity of compounds was enhanced significantly.

Collectively, there was an apparent positive correlation between cell inhibition at 30 μM dosage and lipophilicity as shown in Figure 3G, implying that series **b** compounds might increase their cellular anti-proliferation capacity via an elevated lipophilicity mediated by the Boc group.

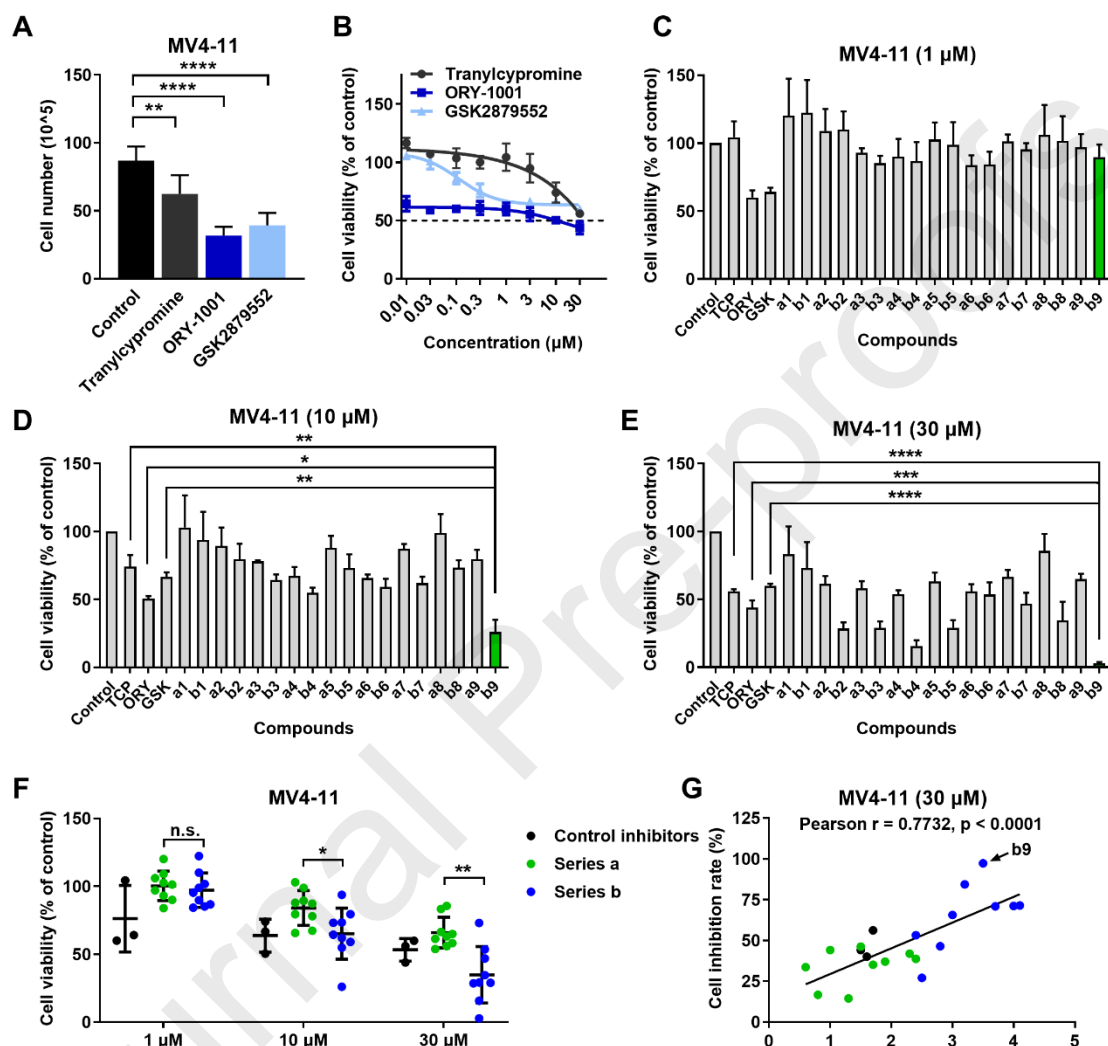


Figure 3. Primary cellular anti-proliferation screening of our synthetic compounds. (A) Cell counting after treatment with three typical TCP-derived LSD1 inhibitors at 5 μM for 8 days. (B) Cell viability after treatment with three inhibitors at gradient dosages for 6 days, determined by MTS assay. (C-E) Preliminary anti-proliferation effect screening of TCP derivatives in MV4-11 cell line via MTS assay at three gradient concentrations, (C) 1 μM , (D) 10 μM and (E) 30 μM . (F) Quantitative anti-proliferation comparison of three known inhibitors, series **a** and series **b** compounds. (G) Correlation analysis of anti-proliferation capacity at 30 μM against CLogP values. All data are representative

of 3 independent experiments and shown as mean \pm SD of triplicates. ^{n.s.} no significance, * $p < 0.05$, ** $p < 0.01$, *** $p < 0.001$, **** $p < 0.0001$ by unpaired, 2-tailed Student's t test.

2.3. Comparison between series a and b compounds at the enzymatic level

Following the preliminary cellular anti-proliferation screening results, we further look at the enzymatic inhibition activity of these two series compounds. Targeting ability against LSD1 was determined by a commercially available LSD1 Inhibitor Screening Assay Kit (#700120, Cayman Chemical, USA), and IC_{50} values in the enzymatic inhibition level were presented in Table 1. Enzymatic curves were shown in Figure S2A-L. All series **a** compounds were better than the parent inhibitor TCP (IC_{50} , 22 μ M) with their IC_{50} values at nanomolar levels, indicating that the introduction of sulfonamide groups significantly enhanced their LSD1 targeting ability. Surprisingly, no significant LSD1 inhibition was observed in all series **b** compounds at 1000 nM (Figure S2M), which was counterintuitive. It seemed that other factors including lipophilicity might play a crucial effect on the anti-proliferation capacity of series **b** compounds.

Table 1. Enzymatic inhibitory activity of the synthetic compounds (IC_{50}).

Series a	IC_{50} (μ M)	Series b	IC_{50} (μ M)
a1	0.3691	b1	> 1
a2	0.2006	b2	> 1
a3	0.4927	b3	> 1
a4	0.4973	b4	> 1
a5	0.2922	b5	> 1
a6	0.8413	b6	> 1
a7	0.1994	b7	> 1
a8	0.2382	b8	> 1
a9	0.1229	b9	> 1

The IC_{50} value indicated the concentration that achieved half inhibition of enzymatic activity.

2.4. The Boc in series b compounds served as a prodrug functional group

Due to the potential lability of Boc to acids, we hypothesized that Boc might be removed within cancerous acid environment to release the real LSD1 inhibitors from

series **b** compounds that did not show detectable inhibition on recombinant LSD1 as shown in Table 1. Therefore, the intracellular LSD1 targeting ability was further tested via thermal shift experiments within cells that were pretreated with each compound. The results, as shown in Figure 4A, indicated that both **a9** and **b9** could stabilize LSD1 protein almost to the same level, confirming that series **b** compounds were able to target cellular LSD1. The action mechanism of TCP compounds to inhibit LSD1 is associated with the generation of amino cation radicals to covalently form an adduct with FAD (Figure 1B).[26, 27] The Boc at the amino site might decrease the nitrogen electronegativity to prevent a cation radical from formation, which was the reason why **b9** did not show apparent enzymatic inhibition of recombinant LSD1. Meanwhile, these results might support our hypothesis that Boc in **b9** might be removed intracellularly to generate the free amine **a9** to act as a real LSD1 inhibitor. To further validate our hypothesis, the Boc in **b9** was changed to a structurally similar pivaloyl group that is not easily removed even under strong acid environment. Thus, compound **c9** was designed and synthesized as shown in Scheme 1B. Cellular thermal shift experiments showed that **c9** did not stabilize LSD1 significantly and moreover its cellular anti-proliferation effect dropped dramatically (Figure 4B and 4C). Meanwhile, **c9** did not inhibit the enzymatic activity of LSD1 in vitro (Figure S3A). Based on these findings, the Boc might serve as a prodrug functional group in TCP derivatives to increase cell permeability and achieve a more effective anti-proliferation effect.

Furthermore, LC-MS/MS was used to investigate the potential intracellular conversion of **b9** to **a9** into a real LSD1 inhibitor. Firstly, such conversion was tested in the culture medium without cells in vitro (Figure S3B). The mass ion signal of **a9** could be detected at pH 6.5 and it substantially increased at pH 6, indicating a possibility that series **b** compounds were able to convert to series **a** compounds under such weak acid conditions. To further validate the in vitro results, MV4-11 cells were treated with 10 μ M of either **a9**, **b9** or **c9** for 3 days and 6 days, and then the cells were lysed and extracted using a solvent system (chloroform : methanol : water = 6 : 3 : 1). The extract was dried via nitrogen blower concentrator and then re-dissolved in 50 %

MeOH/H₂O solution for further LC-MS/MS analysis. The data as shown in Figure 4D and 4E, clearly demonstrated that **a9** could be detected in both samples treated with **a9** and **b9**. The signal of **a9** detected in **b9**-treated cell samples was significantly higher than in **a9**-treated cell samples. Moreover, cellular concentration of **a9** converted from **b9** steadily sustained high while the **a9**-treated samples contained less **a9** after 6 days, likely resulting from the continuous consumption of **a9** by covalently binding to LSD1 co-enzyme FAD as shown in Figure 1B. Meanwhile, **a9** was rarely detected in the **c9**-treated samples as expected. Taken together, the continuous and steady supply of cellular **a9** from **b9** might contribute to its better anti-proliferation capacity, demonstrating the potential of Boc as a prodrug group (Figure 4F).

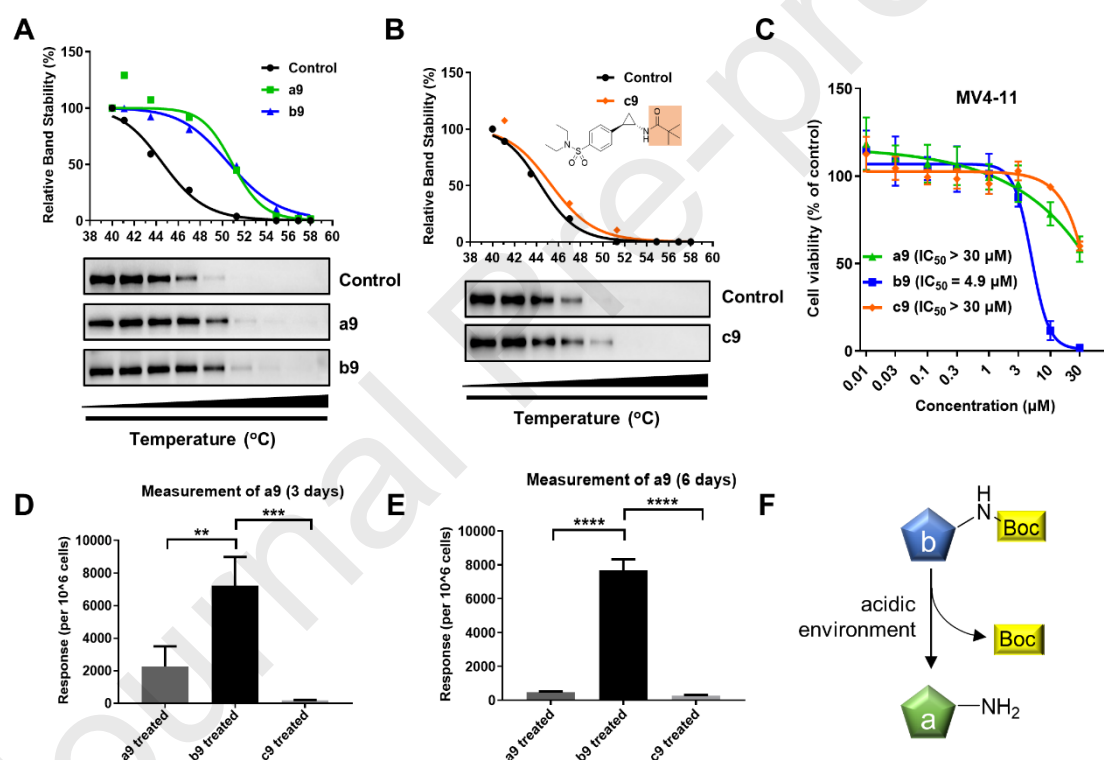


Figure 4. The intracellular LSD1 targeting capacity of series **b** compounds with the Boc group. (A-B) Cellular thermal shift assay of LSD1 in MV4-11 cells treated for 24 h with (A) **a9**, **b9** and (B) **c9** at 5 μM. The level of LSD1 was determined by Western blot. (C) Dose-response curves for the cell viability of MV4-11 cells treated with each drug for 6 days, determined by MTS assay. (D-E) LC-MS/MS detection of **a9** in MV4-11 cells treated with each drug at 10 μM for (D) 3 days and (E) 6 days. (F) Potential conversion mode from **b9** to **a9** within cancerous acid environment. All data are

representative of 3 independent experiments and shown as mean \pm SD. ** $p < 0.01$, *** $p < 0.001$, **** $p < 0.0001$ by One-way ANOVA, Dunnett test.

2.5. Compounds **a9** and **b9** promoted myeloid differentiation

Many examples in the literatures demonstrated that the anticancer effect of LSD1 inhibitors is often involved in the induction of cell differentiation in AML.[26] Since CD11b is regarded as a myeloid differentiation marker, we detected the level of CD11b to compare the effect of compounds **a9**, **b9** and **c9**. The treatment with each of these three compounds for 24 h did not show any impact on MV4-11 cells. However, after 96 h treatment, both **a9** and **b9** significantly induced myeloid differentiation while **c9** did not (Figure 5A-C). Meanwhile, compound **b9** induced more differentiation than **a9**, which might result in the better anti-proliferation activity of series **b** compounds. Similar results were also validated in another AML cell line, HL-60 (Figure 5D-F).

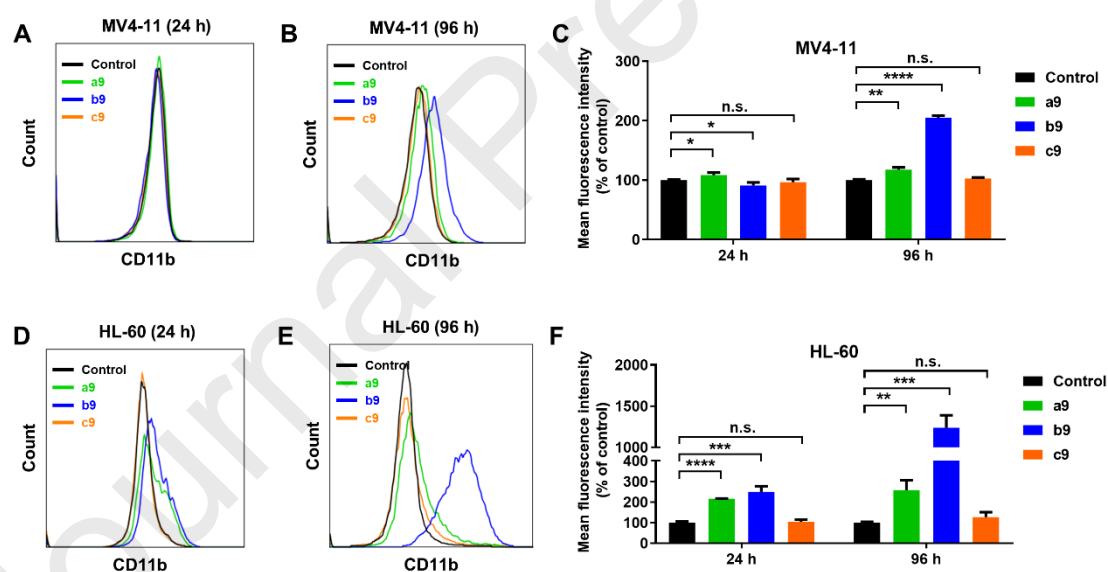


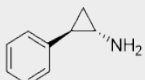
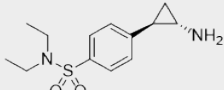
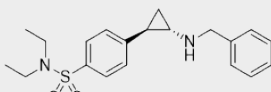
Figure 5. Compounds **a9** and **b9** induced myeloid differentiation. (A, B) Flow cytometry analysis of CD11b on MV4-11 cells treated for (A) 24 h and (B) 96 h with each drug at 10 μ M. (C) Statistic quantitative analysis of the mean CD11b fluorescence intensity from Figure 5A and 5B. (D, E) Flow cytometry analysis of CD11b of HL-60 cells treated for (D) 24 h and (E) 96 h with each drug at 10 μ M. (F) Statistic quantitative analysis of the mean CD11b fluorescence intensity from Figure 5D and 5E. All data are representative of 3 independent experiments and shown as mean \pm SD. n.s. no

significance, *** $p < 0.001$, **** $p < 0.0001$ by unpaired, 2-tailed Student's t test.

2.6. Further lipophilic benzyl installation led to **a10** with potent LSD1 inhibition and improved anticancer capacity

Based on our observation, appropriate lipophilicity was crucial for TCP-based LSD1 inhibitors to enter cancer cells to enact their intracellular biological function. Compared with series **a** compounds, series **b** compounds with a Boc had a properly high CLogP values and displayed better anticancer capacity, likely due to their improved intracellular uptake. Therefore, a lipophilic functional group could be installed at the amino site to increase lipophilicity while remaining enzymatic LSD1 inhibitory potency. Thus, compound **a9** with the best enzymatic LSD1 inhibition was selected to install a benzyl group at the cyclopropane amino site, leading to a new compound **a10** with an elevated CLogP. The introduction of the lipophilic benzyl group surprisingly improved the cell growth inhibition and LSD1 targeting capacity (Table 2 and Figure S4). Notably, **a10** showed better selectivity against LSD1 over other homologous enzymes MAO-A and MAO-B. Meanwhile, the cellular anti-proliferation capacity of **b10** dropped compared to the parental compound **b9**, implying that too high lipophilicity (CLogP > 5) might impair cell permeability of **b10** although **b10** was able to bind to cellular LSD1 as demonstrated in the cellular thermal shift experiment (Table S2 and Figure S5A). Since **a10** showed the best potency against recombinant LSD1 although it inhibited MV4-11 at a slightly higher IC₅₀ concentration compared to **b10** (Figure S5B), **a10** was chosen for further biological studies. Cell counting experiments confirmed that **a10** significantly blocked cell growth at 5 μ M after 6 days of treatment (Figure S5C). Moreover, two other AML cell lines Kasumi-1 and BaF3/ITD also displayed good anti-proliferation responses to the treatment of **a10** (Figure S5D). The direct outcome of LSD1 inhibition was an elevation of H3K4 and H3K9 methylation levels. Indeed, our experiment confirmed that the degrees of H3K4me1, H3K4me2 and H3K9me2 increased significantly after a treatment with **a10**, especially at 10 μ M (Figure 6A and 6B). Thermal shift experiment also verified that **a10** could bind to cellular LSD1 to prevent its thermal destabilization (Figure 6C).

Table 2. Enzymatic activity (IC₅₀), cell growth inhibition and CLogP of TCP, **a9**, and **a10**.

Compounds	Structure	IC ₅₀ (μM)				CLogP
		Cell Growth	LSD1	MAO-A	MAO-B	
TCP		> 30	22 ^a	0.2691	0.5067	1.5
a9		> 30	0.1229	0.8067	0.8975	1.7
a10		15.4	0.0290	0.5255	0.7017	3.9

The IC₅₀ value indicated the concentration that achieved half inhibition of either cell growth or enzymatic activity. CLogP values were analyzed via ChemDraw. ^a Reported in the commercial LSD1 Inhibitor Screening Assay Kit.

Since **a10** inhibited LSD1 both extracellularly and intracellularly, the consequent effect on cell cycle and cell differentiation was tested. After 24 hour treatment, **a10** blocked the cell cycle at G0/G1 phase along with the proportional decrease at S and G2/M phase (Figure 6D). Three reported LSD1 inhibitors required longer time to cause a substantial cell cycle arrest (Figure S5E), whereas **a10** already caused more AML cells death. CD11b, a marker of myeloid differentiation, was also examined. The four compounds did not exhibit an obvious impact on CD11b expression in MV4-11 cells treated for a short 24 h time. However, after 96 hour treatment, **a10** substantially increased the level of CD11b, better than the other three known LSD1 inhibitors (Figure 6E). The induction of myeloid differentiation was also validated in HL60 cell line (Figure S5F). Taken together, compound **a10** targeted LSD1 and subsequently prevented cell growth via cell cycle blockade and myeloid differentiation promotion.

The combination of two drugs is often employed to increase their pharmacological efficacy.[38, 39] Examples in the literature have demonstrated that LSD1 inhibitors in a combination with the clinical drug ATRA exhibited better anticancer effects.[13, 37] Our synthetic compound **a10** was further investigated in a co-treatment with ATRA,

and indeed such a combination achieved a synergistic anti-proliferation effect towards MV4-11 cells via MTS assay (Figure 6F, 6G and Figure S5G).

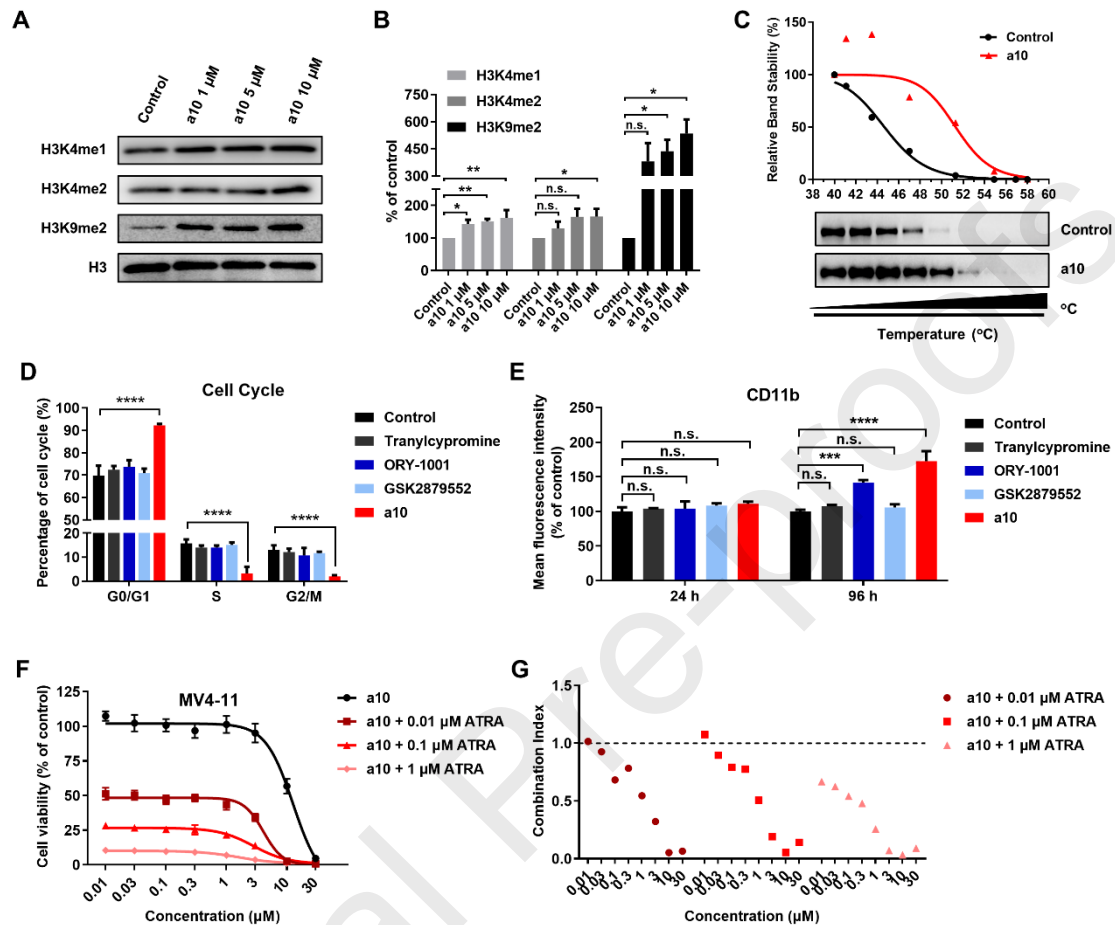


Figure 6. Compound **a10** caused cell cycle blockade, induced myeloid differentiation and exhibited a synergistic effect with the clinical drug ATRA in MV4-11 cell line. (A) Western blot of LSD1 methylated markers treated with **a10** at various concentrations for 24 h. (B) Statistical analysis of the methylation levels in A (Student's t test, unpaired, 2-tailed). (C) Thermal shift assay of intracellular LSD1 with **a10** at 5 μM for 24 h. (D) Flow cytometry analysis of cell cycle after 24 hours treatment with each drug at 10 μM (One-way ANOVA, Dunnett test). (E) Flow cytometry analysis of CD11b after treatment with each drug at 10 μM for 24 h and 96 h (One-way ANOVA, Dunnett test). (F) Dose-response curves of cells co-treated with **a10** at various concentrations and ATRA at indicated concentrations for 6 days. (G) Combination index (CI) of combinations of **a10** and ATRA, analyzed by Calcsyn Software. CI less than 1 means

a synergistic effect. All data are representative of 3 independent experiments and shown as mean \pm SD. ^{n.s.} no significance, * $p < 0.05$, ** $p < 0.01$, *** $p < 0.001$, **** $p < 0.0001$.

3. Conclusions

In our present work, a new series of TCP-based LSD1 inhibitors were developed and evaluated against AML. The introduction of sulfonamide groups in TCP benzene ring site substantially increased the LSD1 inhibition potency. Meanwhile, our work demonstrated that an appropriate lipophilicity and potent LSD1 inhibition contributed to the improved anti-proliferation effect of LSD1 inhibitors towards AML cell lines. The lipophilic Boc group installed in the polar TCP derivatives benefited the drug cellular uptake and could be removed to release the real LSD1 inhibitors under acidic microenvironment in cancer cells. Cellular protein thermal shift experiments further verified that the best anticancer Boc-attached TCP derivative **b9** stabilized intracellular LSD1 although it did not inhibit the recombinant enzyme. Moreover, the mass spectroscopy further confirmed the intracellular release of the real LSD1 inhibitor **a9** from **b9**. Finally, a novel compound **a10** bearing an appropriate lipophilicity was developed, and it substantially inhibited LSD1 and exhibited a good anticancer capacity in several AML cell lines. **a10** may provide a new structural scaffolding to develop more potent LSD1 inhibitors for the therapeutic treatment of acute myeloid leukemia.

4. Experimental section

4.1. Chemistry

4.1.1. General information

Reagents and solvents were commercially available and used without further purification. All nuclear magnetic resonance (NMR) spectra, including ^1H NMR and ^{13}C NMR spectra, were recorded on a Bruker Avance 400 MHz and 100 MHz spectrometer with TMS as an internal standard. Chemical shifts were exhibited in parts per million (δ , ppm) and referenced to CDCl_3 with 7.26 for ^1H and 77.16 for ^{13}C , and to methanol- d_4 with 3.31 for ^1H and 49.00 for ^{13}C . High-resolution mass spectra (HRMS)

were recorded on a Shimadzu Micromass Q-T of Micromass spectrometer by electrospray ionization (ESI). Agilent 1100 HPLC system equipped with an Eclipse XDB-C18 column was used to determine the purity of all final compounds. The flow rate of HPLC was set at 1 mL/min and the gradient elution was run for 15 min, from 10 % MeOH/H₂O to 90 % MeOH/H₂O for 8 min and 90 % MeOH/H₂O for another 7 min. In addition, 1 % formic acid was added to the methanol to elevate the solubility of free amine compounds.

4.1.2. The procedures for synthesis of series a and b compounds

The appropriate triethyl phosphonoacetate (4.11 g, 1.1 equiv) was dissolved in 8 mL of anhydrous 1,4-dioxane (8 mL), and then *n*-BuLi (1.23 g, 1.2 equiv) was added at 0 °C carefully. After stirring for 30 min, 2-phenyloxirane (2.0 g, 1.0 equiv) was added, and then the reaction mixture was subjected to microwave at 135 °C for 1 h. The reaction was stopped using aqueous saturated NH₄Cl, and the mixture was extracted with EtOAc. The organic phases were washed with brine, dried over Na₂SO₄ and finally purified with column chromatography (PE/EtOAc = 50:1) to obtain **2** as a red oil (2.87 g, 91 % yield). Then chlorosulfonic acid (12.5 equiv) was dissolved in anhydrous CH₂Cl₂ (20 mL), and then **2** (2.87 g, 1.0 equiv) in anhydrous CH₂Cl₂ (5 mL) was dropped into the mixture over a period of 1 h at 0 °C. The reaction continued for another 2 h at room temperature. The mixture was finally extracted with CH₂Cl₂ three times and purified via column chromatography (PE/EtOAc = 5:1) to obtain **3** as a yellow oil (2.79 g, 64 % yield). Then a series of amines were introduced at the sulfonyl group side and all compounds shared the following general synthetic procedure.

Compound **3** (1.0 equiv) was sufficiently dissolved in anhydrous CH₂Cl₂, then each type of amine (1.2 equiv) and DIPEA (2.0 equiv) was added at 0 °C respectively. The reaction was stirred at room temperature for 2 h to obtain **4**. Compound **4** (1.0 equiv) was dissolved in THF/H₂O (3:1) and then LiOH (2.0 equiv) was added. The reaction continued for 12 h at room temperature to get **5**. DPPA (1.2 equiv) and Et₃N (1.2 equiv) were added dropwise at 0 °C into the solution of **5** (1.0 equiv) in anhydrous THF. The reaction mixture was stirred for 2.5 h at room temperature, and extracted with EtOAc

and purified with column chromatography to get **6**. The solution of **6** (1.0 equiv) in *t*-BuOH was refluxed at 110 °C for 12 h to finally obtain series **b** compounds **b1-b9**.

Deprotection of Boc group under an acidic condition gave compounds **a1-a9**. Series **b** compound was weighed into the bottle, and a HCl solution in methanol was added at 0 °C carefully. The reaction mixture was stirred at room temperature for 2 h to acquire series **a** compound.

4.1.3. The procedure for synthesis of **c9**

Compound **c9** was obtained from **a9**. To a solution of **a9** (138.4 mg, 1.0 equiv) in anhydrous CH₂Cl₂ (2 mL), DIPEA (276.8 μL, 3.5 equiv) was added at 0 °C carefully. After stirring for 5 minutes, pivaloyl chloride (83.9 μL, 1.5 equiv) was added dropwise and the reaction continued at room temperature for 2 h. The mixture was extracted with EtOAc and the organic phases were washed with brine, dried over Na₂SO₄ and finally purified with column chromatography (PE/EtOAc = 3:1) to obtain **c9** as a white solid (43 mg, 27 % yield).

4.1.4. The procedures for synthesis of **a10** and **b10**

Compounds **a10** and **b10** were obtained from **b9**. To a solution of **b9** (50 mg, 1.0 equiv) in anhydrous THF at 0 °C was added NaH (8 mg, 1.5 equiv). The reaction mixture was stirred for 30 min, and then benzyl bromide (24 μL, 1.2 equiv) was added. The reaction mixture was then warmed to room temperature and stirred for 2 h. The mixture was extracted with EtOAc and the organic phases were washed with brine, dried over Na₂SO₄ and finally purified with column chromatography (PE/EtOAc = 8:1) to obtain **b10** as a white solid (30 mg, 48 % yield). Compound **b10** (25 mg, 1.0 equiv) was weighed into the bottle, and a HCl solution in methanol was added at 0 °C carefully. The reaction mixture was stirred at room temperature for 2 h to acquire **a10** as a yellow solid (10 mg, 46 % yield) after the solvent was removed under a vacuum.

4-(2-Aminocyclopropyl)-N-ethylbenzenesulfonamide (a1)

Yellow solid, 91 % yield, 96 % purity. ¹H NMR (400 MHz, methanol-*d*₄) δ 7.78 (d, *J* = 8.0 Hz, 2H), 7.37 (d, *J* = 8.1 Hz, 2H), 3.00-2.93 (m, 1H), 2.87 (q, *J* = 7.2 Hz, 2H),

2.51 (m, 1H), 1.59-1.49 (m, 1H), 1.43 (m, 1H), 1.04 (t, $J = 7.2$ Hz, 3H). ^{13}C NMR (100 MHz, methanol- d_4) δ 145.1, 140.3, 128.4, 128.1, 39.0, 32.4, 22.4, 15.2, 14.5. HRMS (ESI): m/z calcd for $\text{C}_{11}\text{H}_{16}\text{N}_2\text{O}_2\text{S}$ (M+H) $^+$, 241.1005; found, 241.1000.

Tert-butyl (2-(4-(N-ethylsulfamoyl)phenyl)cyclopropyl)carbamate (b1).

White solid, 72 % yield, 99 % purity. ^1H NMR (400 MHz, methanol- d_4) δ 7.72 (d, $J = 8.4$ Hz, 2H), 7.29 (d, $J = 8.4$ Hz, 2H), 2.86 (q, $J = 7.3$ Hz, 2H), 2.72 (m, 1H), 2.10-2.02 (m, 1H), 1.43 (s, 9H), 1.25 (t, $J = 7.0$ Hz, 2H), 1.04 (t, $J = 7.3$ Hz, 3H). ^{13}C NMR (100 MHz, methanol- d_4) δ 159.0, 148.2, 139.1, 128.0, 127.6, 39.0, 34.6, 28.7, 25.7, 17.1, 15.2. HRMS (ESI): m/z calcd for $\text{C}_{16}\text{H}_{24}\text{N}_2\text{O}_4\text{S}$ (M-H) $^-$, 339.1384; found, 339.1377.

4-(2-Aminocyclopropyl)-N-phenethylbenzenesulfonamide (a2).

Yellow solid, 92 % yield, 98 % purity. ^1H NMR (400 MHz, methanol- d_4) δ 7.70 (d, $J = 8.3$ Hz, 2H), 7.32 (d, $J = 8.3$ Hz, 2H), 7.18 (m, 2H), 7.11 (m, 1H), 7.06 (d, $J = 6.9$ Hz, 2H), 3.03-2.96 (m, 2H), 2.95-2.89 (m, 1H), 2.70-2.63 (m, 2H), 2.52 (m, 1H), 1.58-1.50 (m, 1H), 1.41-1.32 (m, 1H). ^{13}C NMR (100 MHz, methanol- d_4) δ 145.1, 140.3, 139.9, 129.7, 129.5, 128.3, 128.1, 127.4, 45.6, 37.1, 32.4, 22.4, 14.5. HRMS (ESI): m/z calcd for $\text{C}_{17}\text{H}_{20}\text{N}_2\text{O}_2\text{S}$ (M+H) $^+$, 317.1318; found, 317.1333.

Tert-butyl (2-(4-(N-phenethylsulfamoyl)phenyl)cyclopropyl)carbamate (b2).

White solid, 64 % yield, 100 % purity. ^1H NMR (400 MHz, methanol- d_4) δ 7.70 (d, $J = 8.4$ Hz, 2H), 7.22-7.28 (m, 4H), 7.17 (d, $J = 7.2$ Hz, 1H), 7.10 (d, $J = 7.0$ Hz, 2H), 3.04 (t, $J = 7.5$ Hz, 2H), 2.75-2.67 (m, 3H), 2.09-2.00 (m, 1H), 1.43 (s, 9H), 1.31-1.21 (m, 2H). ^{13}C NMR (100 MHz, CDCl_3) δ 156.4, 146.5, 137.8, 137.3, 128.9, 127.3, 127.0, 126.9, 80.0, 44.3, 35.9, 28.5, 17.0. HRMS (ESI): m/z calcd for $\text{C}_{22}\text{H}_{28}\text{N}_2\text{O}_4\text{S}$ (M-H) $^-$, 415.1697; found, 415.1689.

4-(2-Aminocyclopropyl)-N-cyclohexylbenzenesulfonamide (a3).

Pale yellow solid, 76 % yield, 99 % purity. ^1H NMR (400 MHz, methanol- d_4) δ 7.80 (d, $J = 8.0$ Hz, 2H), 7.36 (d, $J = 8.0$ Hz, 2H), 2.97 (m, 1H), 2.50 (m, 1H), 1.65 (m, 4H), 1.57-1.50 (m, 2H), 1.44 (m, 1H), 1.24-1.05 (m, 6H). ^{13}C NMR (100 MHz, methanol- d_4) δ 144.9, 141.9, 128.2, 128.0, 53.9, 34.9, 32.5, 26.3, 26.0, 22.4, 14.6. HRMS (ESI):

m/z calcd for C₁₅H₂₂N₂O₂S (M+H)⁺, 295.1475; found, 295.1483.

Tert-butyl (2-(4-(N-cyclohexylsulfamoyl)phenyl)cyclopropyl)carbamate (b3).

White solid, 62 % yield, 100 % purity. ¹H NMR (400 MHz, CDCl₃) δ 7.75 (d, *J* = 8.3 Hz, 2H), 7.21 (d, *J* = 7.7 Hz, 2H), 4.94 (s, 1H), 4.68 (d, *J* = 7.5 Hz, 1H), 3.15-3.03 (m, 1H), 2.77 (m, 1H), 2.09 (m, 1H), 1.66-1.57 (m, 2H), 1.54-1.46 (m, 2H), 1.43 (s, 9H), 1.28-1.06 (m, 8H). ¹³C NMR (100 MHz, CDCl₃) δ 146.2, 138.9, 127.1, 127.0, 80.0, 52.7, 34.0, 29.8, 28.5, 25.3, 24.7, 17.0. HRMS (ESI): m/z calcd for C₂₀H₃₀N₂O₄S (M+H)⁺, 395.1999; found, 395.1984.

4-(2-Aminocyclopropyl)-N-(tert-butyl)benzenesulfonamide (a4).

Yellow solid, 97 % yield, 96 % purity. ¹H NMR (400 MHz, methanol-*d*₄) δ 7.81 (d, *J* = 8.2 Hz, 2H), 7.34 (d, *J* = 8.1 Hz, 2H), 3.31 (s, 1H), 2.99-2.91 (m, 1H), 2.48 (m, 1H), 1.58-1.47 (m, 1H), 1.43 (m, 1H), 1.16 (s, 9H). ¹³C NMR (100 MHz, methanol-*d*₄) δ 144.7, 144.0, 128.2, 127.8, 54.8, 32.4, 30.4, 22.4, 14.6. HRMS (ESI): m/z calcd for C₁₃H₂₀N₂O₂S (M+H)⁺, 269.1318; found, 269.1310.

Tert-butyl (2-(4-(N-(tert-butyl)sulfamoyl)phenyl)cyclopropyl)carbamate (b4).

White solid, 44 % yield, 99 % purity. ¹H NMR (400 MHz, CDCl₃) δ 7.76 (d, *J* = 8.4 Hz, 2H), 7.19 (d, *J* = 8.1 Hz, 2H), 4.98 (s, 1H), 4.90 (s, 1H), 2.75 (m, 1H), 2.07 (m, 1H), 1.43 (s, 9H), 1.23 (m, 1H), 1.20 (m, 1H), 1.19 (s, 9H). ¹³C NMR (100 MHz, CDCl₃) δ 156.5, 145.9, 141.1, 127.1, 126.8, 80.0, 54.7, 33.3, 30.2, 28.5, 25.4, 16.9. HRMS (ESI): m/z calcd for C₁₈H₂₈N₂O₄S (M-H)⁻, 367.1697; found, 367.1684.

4-(2-Aminocyclopropyl)-N-phenylbenzenesulfonamide (a5).

White solid, 82 % yield, 96 % purity. ¹H NMR (400 MHz, methanol-*d*₄) δ 7.69 (d, *J* = 7.8 Hz, 2H), 7.27 (d, *J* = 7.9 Hz, 2H), 7.19 (t, *J* = 7.6 Hz, 2H), 7.09-7.01 (m, 3H), 2.94-2.87 (m, 1H), 2.46-2.38 (m, 1H), 1.52-1.45 (m, 1H), 1.39 (d, *J* = 6.9 Hz, 1H). ¹³C NMR (100 MHz, methanol-*d*₄) δ 145.5, 139.4, 138.9, 130.1, 128.6, 127.9, 125.7, 122.2, 32.4, 22.4, 14.6. HRMS (ESI): m/z calcd for C₁₅H₁₆N₂O₂S (M+H)⁺, 289.1005; found, 289.0995.

Tert-butyl (2-(4-(N-phenylsulfamoyl)phenyl)cyclopropyl)carbamate (b5).

White solid, 26 % yield, 99 % purity. ^1H NMR (400 MHz, CDCl_3) δ 7.64 (d, $J = 8.2$ Hz, 2H), 7.22 (d, $J = 7.7$ Hz, 2H), 7.13 (m, 3H), 7.05 (d, $J = 7.9$ Hz, 2H), 6.73 (s, 1H), 4.86 (s, 1H), 2.73 (m, 1H), 2.04 (m, 1H), 1.42 (s, 9H), 1.24 – 1.16 (m, 2H). ^{13}C NMR (100 MHz, methanol- d_4) δ 159.0, 148.6, 139.0, 138.2, 130.1, 128.2, 127.4, 125.7, 122.2, 80.4, 34.6, 28.7, 25.7, 17.1. HRMS (ESI): m/z calcd for $\text{C}_{20}\text{H}_{24}\text{N}_2\text{O}_4\text{S}$ ($\text{M}+\text{H}$) $^+$, 389.1530; found, 389.1531.

4-(2-Aminocyclopropyl)-N-(pyridin-2-yl)benzenesulfonamide (a6).

Yellow solid, 89 % yield, 95 % purity. ^1H NMR (400 MHz, methanol- d_4) δ 8.25 (d, $J = 5.7$ Hz, 1H), 8.13 (t, $J = 7.9$ Hz, 1H), 7.88 (d, $J = 8.1$ Hz, 2H), 7.45-7.30 (m, 4H), 2.92 (m, 1H), 2.49 (m, 1H), 1.56-1.49 (m, 1H), 1.38 (dd, $J = 14.0, 6.8$ Hz, 1H). ^{13}C NMR (100 MHz, methanol- d_4) δ 150.3, 146.9, 141.7, 139.2, 128.5, 120.2, 117.6, 101.3, 32.5, 22.4, 14.7. HRMS (ESI): m/z calcd for $\text{C}_{14}\text{H}_{15}\text{N}_3\text{O}_2\text{S}$ ($\text{M}+\text{H}$) $^+$, 290.0958; found, 290.0958.

Tert-butyl (2-(4-(N-(pyridin-2-yl)sulfamoyl)phenyl)cyclopropyl)carbamate (b6).

Yellow solid, 50 % yield, 99 % purity. ^1H NMR (400 MHz, CDCl_3) δ 8.32 (d, $J = 5.9$ Hz, 1H), 7.79 (d, $J = 8.2$ Hz, 2H), 7.64 (t, $J = 7.3$ Hz, 1H), 7.37 (d, $J = 8.9$ Hz, 1H), 7.17 (d, $J = 7.9$ Hz, 2H), 6.78 (t, $J = 6.4$ Hz, 1H), 4.89 (s, 1H), 2.72 (m, 1H), 2.05 (m, 1H), 1.42 (s, 9H), 1.27-1.15 (m, 2H). ^{13}C NMR (100 MHz, CDCl_3) δ 155.4, 145.8, 142.5, 140.2, 139.4, 127.0, 126.9, 115.4, 113.9, 33.1, 28.5, 25.3, 16.9. HRMS (ESI): m/z calcd for $\text{C}_{19}\text{H}_{23}\text{N}_3\text{O}_4\text{S}$ ($\text{M}+\text{H}$) $^+$, 390.1482; found, 390.1468.

2-(4-(Morpholinosulfonyl)phenyl)cyclopropan-1-amine (a7).

Pale yellow solid, 91 % yield, 95 % purity. ^1H NMR (400 MHz, methanol- d_4) δ 7.72 (d, $J = 7.9$ Hz, 2H), 7.43 (d, $J = 8.0$ Hz, 2H), 3.72-3.66 (m, 4H), 2.99 (m, 1H), 2.96-2.91 (m, 4H), 2.55-2.47 (m, 1H), 1.59-1.50 (m, 1H), 1.46 (dd, $J = 13.8, 6.9$ Hz, 2H). ^{13}C NMR (100 MHz, methanol- d_4) δ 146.0, 142.6, 129.4, 128.3, 67.2, 47.4, 32.5, 22.4, 14.7. HRMS (ESI): m/z calcd for $\text{C}_{13}\text{H}_{18}\text{N}_2\text{O}_3\text{S}$ ($\text{M}+\text{H}$) $^+$, 283.1111; found, 283.1104.

Tert-butyl (2-(4-(morpholinosulfonyl)phenyl)cyclopropyl)carbamate (b7).

Yellow solid, 37 % yield, 97 % purity. ^1H NMR (400 MHz, CDCl_3) δ 7.63 (d, $J =$

7.9 Hz, 2H), 7.27 (d, $J = 7.8$ Hz, 2H), 4.92 (s, 1H), 3.76-3.68 (m, 4H), 2.99-2.91 (m, 4H), 2.77 (m, 1H), 2.11 (m, 1H), 1.44 (s, 9H), 1.25 (m, 2H). ^{13}C NMR (100 MHz, CDCl_3) δ 156.3, 147.0, 132.6, 128.1, 127.1, 66.2, 46.1, 28.5, 17.0. HRMS (ESI): m/z calcd for $\text{C}_{18}\text{H}_{26}\text{N}_2\text{O}_5\text{S}$ ($\text{M}+\text{H}$) $^+$, 383.1635; found, 383.1621.

2-(4-(Pyrrolidin-1-ylsulfonyl)phenyl)cyclopropan-1-amine (a8).

Yellow solid, 94 % yield, 97 % purity. ^1H NMR (400 MHz, methanol- d_4) δ 7.72 (d, $J = 8.2$ Hz, 2H), 7.38 (d, $J = 8.2$ Hz, 2H), 3.16 (t, $J = 6.7$ Hz, 4H), 2.98-2.91 (m, 1H), 2.51 (m, 1H), 1.73-1.64 (m, 4H), 1.58-1.50 (m, 1H), 1.40 (m, 1H). ^{13}C NMR (100 MHz, methanol- d_4) δ 145.6, 136.6, 129.0, 128.2, 32.5, 26.2, 22.4, 14.6. HRMS (ESI): m/z calcd for $\text{C}_{13}\text{H}_{18}\text{N}_2\text{O}_2\text{S}$ ($\text{M}+\text{H}$) $^+$, 267.1162; found, 267.1156.

Tert-butyl (2-(4-(pyrrolidin-1-ylsulfonyl)phenyl)cyclopropyl)carbamate (b8).

White solid, 57 % yield, 99 % purity. ^1H NMR (400 MHz, CDCl_3) δ 7.71 (d, $J = 8.3$ Hz, 1H), 7.24 (d, $J = 8.2$ Hz, 1H), 3.21 (t, $J = 6.7$ Hz, 2H), 2.76 (m, 1H), 2.14-2.05 (m, 1H), 1.78-1.71 (m, 4H), 1.44 (s, 9H), 1.27-1.20 (m, 2H). ^{13}C NMR (100 MHz, CDCl_3) δ 156.5, 146.4, 134.5, 127.8, 126.9, 80.0, 48.0, 28.5, 25.3, 16.9. HRMS (ESI): m/z calcd for $\text{C}_{18}\text{H}_{26}\text{N}_2\text{O}_4\text{S}$ ($\text{M}+\text{H}$) $^+$, 367.1686; found, 367.1678.

4-(2-Aminocyclopropyl)-N,N-diethylbenzenesulfonamide (a9).

Yellow solid, 58 % yield, 99 % purity. ^1H NMR (400 MHz, methanol- d_4) δ 7.71 (d, $J = 8.0$ Hz, 2H), 7.34 (d, $J = 8.1$ Hz, 2H), 3.18 (q, $J = 7.1$ Hz, 4H), 2.95-2.88 (m, 1H), 2.48 (m, 1H), 1.56-1.47 (m, 1H), 1.39 (m, 1H), 1.07 (t, $J = 7.1$ Hz, 6H). ^{13}C NMR (100 MHz, CDCl_3) δ 143.5, 138.9, 127.8, 127.6, 42.5, 14.5, 14.2. HRMS (ESI): m/z calcd for $\text{C}_{13}\text{H}_{20}\text{N}_2\text{O}_2\text{S}$ ($\text{M}+\text{H}$) $^+$, 269.1318; found, 269.1310.

Tert-butyl (2-(4-(N,N-diethylsulfamoyl)phenyl)cyclopropyl)carbamate (b9).

White solid, 47 % yield, 99 % purity. ^1H NMR (400 MHz, CDCl_3) δ 7.68 (d, $J = 8.4$ Hz, 2H), 7.21 (d, $J = 8.2$ Hz, 2H), 3.20 (q, $J = 7.1$ Hz, 4H), 2.75 (m, 1H), 2.13-2.03 (m, 1H), 1.44 (s, 9H), 1.26-1.18 (m, 2H), 1.12 (t, $J = 7.1$ Hz, 6H). ^{13}C NMR (100 MHz, CDCl_3) δ 156.3, 146.0, 137.8, 127.2, 126.9, 80.0, 42.2, 33.2, 28.5, 25.3, 16.9, 14.4. HRMS (ESI): m/z calcd for $\text{C}_{18}\text{H}_{28}\text{N}_2\text{O}_4\text{S}$ ($\text{M}+\text{H}$) $^+$, 369.1843; found, 369.1846.

***N*-(2-(4-(*N,N*-diethylsulfamoyl)phenyl)cyclopropyl)pivalamide (c9).**

White solid, 27 % yield, 95 % purity. ¹H NMR (400 MHz, CDCl₃) δ 7.69 (d, *J* = 8.3 Hz, 2H), 7.28 (d, *J* = 8.3 Hz, 2H), 5.90 (s, 1H), 3.20 (q, *J* = 7.1 Hz, 4H), 2.88 (m, 1H), 2.05 (m, 1H), 1.29 (m, 2H), 1.20 (s, 9H), 1.12 (t, *J* = 7.1 Hz, 6H). ¹³C NMR (100 MHz, CDCl₃) δ 180.0, 145.8, 137.9, 127.2, 127.2, 42.2, 38.7, 32.9, 27.6, 25.2, 16.4, 14.3. HRMS (ESI): *m/z* calcd for C₁₈H₂₈N₂O₃S (M+H)⁺, 353.1893; found, 353.1885.

***4*-(2-(Benzylamino)cyclopropyl)-*N,N*-diethylbenzenesulfonamide (a10).**

Yellow solid, 46 % yield, 97 % purity. ¹H NMR (400 MHz, CDCl₃) δ 7.65 (d, *J* = 7.8 Hz, 2H), 7.53 (s, 2H), 7.34 (m, 3H), 7.04 (d, *J* = 7.9 Hz, 2H), 4.12 (m, 2H), 3.20 (q, *J* = 7.1 Hz, 4H), 2.75 (m, 1H), 2.55 (m, 1H), 1.25 (m, 2H), 1.11 (t, *J* = 7.1 Hz, 6H). ¹³C NMR (125 MHz, CDCl₃) δ 142.9, 139.1, 131.6, 130.0, 129.8, 129.6, 128.0, 127.7, 53.6, 42.5, 29.8, 14.5. HRMS (ESI): *m/z* calcd for C₂₀H₂₆N₂O₂S (M+H)⁺, 359.1788; found, 359.1777.

***Tert*-butyl benzyl(2-(4-(*N,N*-diethylsulfamoyl)phenyl)cyclopropyl)carbamate (b10).**

White solid, 48 % yield, 96 % purity. ¹H NMR (400 MHz, CDCl₃) δ 7.66 (d, *J* = 8.3 Hz, 2H), 7.33-7.28 (m, 2H), 7.23 (t, *J* = 6.5 Hz, 3H), 7.16-7.09 (m, 2H), 4.62 (d, *J* = 15.2 Hz, 1H), 4.35 (d, *J* = 15.4 Hz, 1H), 3.20 (q, *J* = 7.1 Hz, 4H), 2.73-2.66 (m, 1H), 2.18 (m, 1H), 1.41 (s, 9H), 1.20 (m, 2H), 1.10 (t, *J* = 7.2 Hz, 6H). ¹³C NMR (125 MHz, CDCl₃) δ 146.2, 138.6, 137.8, 130.6, 128.7, 127.6, 127.3, 127.1, 126.7, 80.4, 42.1, 39.6, 28.5, 14.2. HRMS (ESI): *m/z* calcd for C₂₅H₃₄N₂O₄S (M+H)⁺, 459.2312; found, 459.2312

4.2. Biological assays**4.2.1. Cell culture**

AML cell lines MV4-11, HL-60, THP-1, U937, ML1, MOLM-13 and BaF3/ITD were obtained from American Type Culture Collection (Rockville, MD, USA) and maintained in RPMI-1640 medium (Gibco, Carlsbad, CA, USA) supplemented with 10 % fetal bovine serum (FBS, Biological Industries, Israel). Kasumi-1 cell line was kindly provided by Stem Cell Bank, Chinese Academy of Sciences and cultured in RPMI 1640

medium containing 20 % FBS, 1 % GlutaMAX™-I (Gibco, Carlsbad, CA, USA) and 1 % sodium pyruvate (Gibco, Carlsbad, CA, USA). All cell lines were incubated at 37 °C supplied with 5 % carbon dioxide.

4.2.2. Cell proliferation assays through MTS and cell counting

Cell viability was determined by MTS assay. MTS (3-(4,5-dimethylthiazol-2-yl)-5-(3-carboxymethoxyphenyl)-2-(4-sulfophenyl)-2H-tetrazolium, inner salt) can be reduced by dehydrogenase enzymes in metabolically active cells into a colored formazan product that is soluble in the medium and is directly detected by visible light absorption at 490 nm with a 96-well plate reader. Briefly, cells were plated at 5000 cells per well in round bottom 96-well plates in triplicate. After 2 h of incubation at the 37 °C incubator, the cells were exposed to gradient concentrations of typical LSD1 inhibitors or our synthetic compounds for 6 days. At the end of the incubation, 20 µL of MTS solution (2 mg/mL) was added into each well and the cells were incubated at 37 °C supplied with 5 % carbon dioxide for 4 h. Then the optical density value (OD) was determined at 490 nm wavelength with a BioTek Gen5 microplate-reader (BioTek Instruments, Winooski, Vermont, USA).

To directly quantify the cell proliferation, cell numbers were counted using a cell counter (Cellometer Auto T4, Nexcelom Bioscience, Lawrence, MA, USA). Briefly, cells were plated at 1×10^5 cells per well in 6-well plates. After 2 h of incubation, the cells were subjected to three typical LSD1 inhibitors (TCP, ORY-1001 and GSK2879552) at 5 µM for 8 days. On the last day, the cells were resuspended thoroughly and counted via the cell counter.

4.2.3. LSD1 enzymatic inhibition measurement

Enzymatic inhibition rate was measured by a commercially available LSD1 Inhibitor Screening Assay Kit (#700120, Cayman Chemical, USA) according to the manufacturer's instructions. In brief, the reagents including diluted assay buffer, LSD1 protein, horseradish peroxidase and fluorometric substrate were added into the plates successively. Then gradient concentrations of our synthetic compounds were added. Finally, the reaction was initiated by the addition of the peptide corresponding to the

first 21 amino acids of N-terminal tail of histone H3 with a di-methylated lysine at residue 4. The plate was covered and incubated at 37 °C for 30 minutes. At the end of the incubation, the plate was read using an excitation wavelength of 530-540 nm and an emission wavelength of 585-595 nm. The enzymatic inhibition rates were calculated by dividing the control group after deduction of the background effect.

4.2.4. Cellular thermal shift assay

Exponential growth phase MV4-11 cells (1×10^6 cells/well) were seeded in a 6-well plate and incubated with compounds either **a9**, **b9**, **c9** or **a10** at 5 μ M for 24 h in the 5 % CO₂ containing incubator at 37 °C. Then, the cells were centrifuged at 1000 rpm for 3 min, washed three times with PBS, resuspended with 1 mL PBS containing 1 % protease inhibitors, and divided equally into eight PCR tubes (100 μ L cell solution per tube). The tubes were treated with gradient temperatures (40 °C-58 °C) for 3 minutes in a PCR thermal cycler, placed at room temperature for 3 minutes and then subjected to snap-freezing in liquid nitrogen for 3 minutes. The above cycles were repeated three times. The thawed cell lysates were centrifuged at 20000 g at 4 °C for 20 minutes, and then the supernatants were collected carefully for further Western Blot analysis.

4.2.5. Detection of **a9** in cell samples via LC-MS/MS

The cells were seeded in a 6-well plate and incubated with compounds either **a9**, **b9** or **c9** at 10 μ M for 3 days and 6 days, respectively. At the end of the incubation, the cells were washed twice with cold saline, lysed and extracted using the solution (chloroform : methanol : water = 6 : 3 : 1). The extract was dried via nitrogen blower concentrator and then re-dissolved in 100 μ L of 50 % MeOH/H₂O solution for LC-MS/MS detection.

Chromatographic separation was performed using an Agilent 1290 Infinity II liquid chromatography system (Agilent, USA) with ZORBAX Eclipse Plus C18 analytical column (2.1 \times 50 mm, 1.8 μ m particle size) (Waters, USA). The flow rate of HPLC was set at 0.4 mL/min and the gradient elution was run for 15 min, from 10 % MeOH/H₂O to 90 % MeOH/H₂O for 10 min and 90 % MeOH/H₂O for another 5 min. The 6495 Triple Quad mass spectrometer (Agilent, USA) with an electrospray ionization (ESI)

interface operated in positive mode was used for the multiple reaction monitoring (MRM) LC-MS/MS analysis. The following precursor and product ion transitions were used for MRM: **a9**, 269.1→115.1, 269.1→162.2. MS data were processed using the Agilent MassHunter Quantitative Analysis (Version B.07.00, Agilent, USA).

4.2.6. Flow cytometric analysis of cell differentiation and cell cycle

Cell differentiation was determined by flow cytometry using anti-CD11b (#553311, BD biosciences, New Jersey, USA). In brief, cells were seeded in the 24-well plate and incubated with different compounds at 10 μ M for 24 h and 96 h. At the end of the incubation, the cells were centrifuged at 800 rpm for 5 minutes to remove dead cells, washed twice with 1 mL cold PBS and then incubated with a solution containing CD11b antibody at 4 °C for 30 minutes. Then, the cells were washed and resuspended with 300 μ L cold PBS for final detection by flow cytometer.

Cell cycle was detected by staining DNA with PI/RNase solution (#550825, BD biosciences, New Jersey, USA) using flow cytometry. Briefly, the cells (1×10^5 for 24 h and 4×10^5 for 96 h treatment) were seeded in the 24-well plate and incubated with either TCP, ORY-1001, GSK2879552 or **a10** at 10 μ M for 24 h and 96 h. At the end of the incubation, the cells were centrifuged at 1000 rpm for 3 min, washed once with 1 mL cold PBS and then resuspended with 500 μ L of 70 % MeOH/H₂O solution for 4 h. After removal of methanol through centrifugation at 1000 rpm for 3 min, the cells were incubated with 300 μ L PI/RNase solution, for 30 minutes at room temperature. At the end of the incubation, the resuspended cell solution was directly tested by flow cytometry.

4.2.7. MAO-A and MAO-B enzymatic inhibition assay

The measurement of MAO-A and MAO-B enzymatic inhibition rates was conducted by the company (Jiangsu Meimian industrial Co., Ltd). In brief, recombinant MAO-A protein (240 μ L), inhibitors (360 μ L) and 100 mM potassium phosphate solution (100 μ L) were added into the tubes sequentially and incubated at 37 °C for 20 min. At the end of the incubation, 10 g/L 5-hydroxytryptamine (100 μ L) was added and incubated at 37 °C for 60 min. Then the reaction was stopped with 60 % HClO₄ (200 μ L). The

reaction product (5- hydroxyindole-3-acetaldehyde) was extracted using butyl acetate (3 mL), centrifuged at 10000 g for 5 min, and the OD value was finally determined at 280 nm wavelength. Similarly, recombinant MAO-B protein (190 μ L), inhibitors (460 μ L) and 100 mM potassium phosphate solution (50 μ L) were added into the tubes sequentially and incubated at 37 °C for 20 min. At the end of the incubation, 98.1 g/L benzylamine (100 μ L) was added and incubated at 37 °C for 60 min. Then the reaction was stopped with 60 % HClO₄ (200 μ L). The reaction product (benzaldehyde) was extracted using cyclohexane (3 mL), centrifuged at 10000 g for 5 min, and the OD value was finally determined at 242 nm wavelength.

4.2.8. Western Blot

The MV4-11 cells (1×10^6 cells/well) were seeded in a 6-well plate and incubated with compound **a9** at 1, 5, or 10 μ M for 24 h in the 5 % CO₂ containing incubator at 37 °C. At the end of the incubation, the cells were centrifuged at 1000 rpm for 3 min, washed with PBS twice. Proteins from the collected cells were extracted in lysis buffer (5 % SDS, 10 mM EDTA, 250 mM NaCl, 10 mM Tris-HCl, pH 7.4), and were subjected to 95 °C heating for 15 min for thorough denaturation. The protein concentrations were measured via Pierce BCA protein assay (#23225, Thermo Fisher, Rockford, IL, USA). Each sample was adjusted to equal protein concentrations with relative quantification methods for Western Blot analysis. Briefly, the samples were subjected to 12 % SDS-PAGE, and then transferred to PVDF membranes (Millipore, Billerica, MA, USA). After that, the proteins on the membranes were probed with primary antibodies and secondary antibodies, and then detected by ECL reagent (#34579, Thermo Fisher, Rockford, IL, USA). The antibodies used for Western Blot analysis, anti-H3 (#4499), anti-H3K4me1 (#5326), anti-H3K4me2 (#9725), anti-H3K9me2 (#4658) and anti-LSD1 (#2139) were purchased from Cell Signaling Technology (Danvers, MA, USA).

Acknowledgment

We are grateful to the grant support from National Natural Science Foundation of China (81672952, 81872440), Guangdong Science and Technology Program

(2017A020215198), and Guangzhou Science and Technology Program (201807010041).

Reference

- [1] C. Duy, M. Teater, F.E. Garrett-Bakelman, T.C. Lee, C. Meydan, J.L. Glass, M. Li, J.C. Hellmuth, H.P. Mohammad, K.N. Smitheman, A.H. Shih, O. Abdel-Wahab, M.S. Tallman, M.L. Guzman, D. Muench, H.L. Grimes, G.J. Roboz, R.G. Kruger, C.L. Creasy, E.M. Paietta, R.L. Levine, M. Carroll, A.M. Melnick, Rational Targeting of Cooperating Layers of the Epigenome Yields Enhanced Therapeutic Efficacy against AML, *Cancer Discov* 9(7) (2019) 872-889.
- [2] T. Wada, D. Koyama, J. Kikuchi, H. Honda, Y. Furukawa, Overexpression of the shortest isoform of histone demethylase LSD1 primes hematopoietic stem cells for malignant transformation, *Blood* 125(24) (2015) 3731-3746.
- [3] M. Cusan, C. SF, M. HP, A. Krivtsov, A. Chramiec, E. Loizou, W. MD, S. KN, T. DG, M. Ye, LSD1 inhibition exerts its anti-leukemic effect by recommissioning PU.1- and C/EBP α -dependent enhancers in AML, *Blood* 131(15) (2018) 1730-1742.
- [4] H.P. Mohammad, O. Barbash, C.L. Creasy, Targeting epigenetic modifications in cancer therapy: erasing the roadmap to cancer, *Nat Med* 25(3) (2019) 403-418.
- [5] A.G. Cochran, A.R. Conery, R.J. Sims, 3rd, Bromodomains: a new target class for drug development, *Nat Rev Drug Discov* 18(8) (2019) 609-628.
- [6] X. Huang, J. Yan, M. Zhang, Y. Wang, Y. Chen, X. Fu, R. Wei, X.L. Zheng, Z. Liu, X. Zhang, H. Yang, B. Hao, Y.Y. Shen, Y. Su, X. Cong, M. Huang, M. Tan, J. Ding, M. Geng, Targeting Epigenetic Crosstalk as a Therapeutic Strategy for EZH2-Aberrant Solid Tumors, *Cell* 175(1) (2018) 186-199.
- [7] Y. Shi, F. Lan, C. Matson, P. Mulligan, J.R. Whetstine, P.A. Cole, R.A. Casero, Y. Shi, Histone demethylation mediated by the nuclear amine oxidase homolog LSD1, *Cell* 119(7) (2004) 941-953.
- [8] W. Sheng, M.W. LaFleur, T.H. Nguyen, S. Chen, A. Chakravarthy, J.R. Conway, Y. Li, H. Chen, H. Yang, P.H. Hsu, E.M. Van Allen, G.J. Freeman, D.D. De Carvalho, H.H. He, A.H. Sharpe, Y. Shi, LSD1 Ablation Stimulates Anti-tumor Immunity and

- Enables Checkpoint Blockade, *Cell* 174(3) (2018) 549-563.
- [9] M.G. Lee, C. Wynder, N. Cooch, R. Shiekhattar, An essential role for CoREST in nucleosomal histone 3 lysine 4 demethylation, *Nature* 437(7057) (2005) 432-435.
- [10] E. Metzger, M. Wissmann, N. Yin, J.M. Muller, R. Schneider, A.H. Peters, T. Gunther, R. Buettner, R. Schule, LSD1 demethylates repressive histone marks to promote androgen-receptor-dependent transcription, *Nature* 437(7057) (2005) 436-439.
- [11] J. Wang, K. Scully, X. Zhu, L. Cai, J. Zhang, G.G. Prefontaine, A. Krones, K.A. Ohgi, P. Zhu, I. Garcia-Bassets, F. Liu, H. Taylor, J. Lozach, F.L. Jayes, K.S. Korach, C.K. Glass, X.D. Fu, M.G. Rosenfeld, Opposing LSD1 complexes function in developmental gene activation and repression programmes, *Nature* 446(7138) (2007) 882-887.
- [12] A.A. Lokken, N.J. Zeleznik-Le, Breaking the LSD1/KDM1A addiction: therapeutic targeting of the epigenetic modifier in AML, *Cancer cell* 21(4) (2012) 451-453.
- [13] T. Schenk, W.C. Chen, S. Gollner, L. Howell, L. Jin, K. Hebestreit, H.U. Klein, A.C. Popescu, A. Burnett, K. Mills, R.A. Casero, Jr., L. Marton, P. Woster, M.D. Minden, M. Dugas, J.C. Wang, J.E. Dick, C. Muller-Tidow, K. Petrie, A. Zelent, Inhibition of the LSD1 (KDM1A) demethylase reactivates the all-trans-retinoic acid differentiation pathway in acute myeloid leukemia, *Nat Med* 18(4) (2012) 605-611.
- [14] Y. Itoh, K. Aihara, P. Mellini, T. Tojo, Y. Ota, H. Tsumoto, V.R. Solomon, P. Zhan, M. Suzuki, D. Ogasawara, A. Shigenaga, T. Inokuma, H. Nakagawa, N. Miyata, T. Mizukami, A. Otaka, T. Suzuki, Identification of SNAIL1 Peptide-Based Irreversible Lysine-Specific Demethylase 1-Selective Inactivators, *J Med Chem* 59(4) (2016) 1531-1544.
- [15] H.M. Liu, F.Z. Suo, X.B. Li, Y.H. You, C.T. Lv, C.X. Zheng, G.C. Zhang, Y.J. Liu, W.T. Kang, Y.C. Zheng, H.W. Xu, Discovery and synthesis of novel indole derivatives-containing 3-methylenedihydrofuran-2(3H)-one as irreversible LSD1 inhibitors, *Eur J Med Chem* 175 (2019) 357-372.
- [16] L.Y. Ma, Y.C. Zheng, S.Q. Wang, B. Wang, Z.R. Wang, L.P. Pang, M. Zhang,

J.W. Wang, L. Ding, J. Li, C. Wang, B. Hu, Y. Liu, X.D. Zhang, J.J. Wang, Z.J. Wang, W. Zhao, H.M. Liu, Design, synthesis, and structure-activity relationship of novel LSD1 inhibitors based on pyrimidine-thiourea hybrids as potent, orally active antitumor agents, *J Med Chem* 58(4) (2015) 1705-1716.

[17] T.E. McAllister, K.S. England, R.J. Hopkinson, P.E. Brennan, A. Kawamura, C.J. Schofield, Recent Progress in Histone Demethylase Inhibitors, *J Med Chem* 59(4) (2016) 1308-1329.

[18] L. Sartori, C. Mercurio, F. Amigoni, A. Cappa, G. Faga, R. Fattori, E. Legnagli, G. Ciossani, A. Mattevi, G. Meroni, L. Moretti, V. Cecatiello, S. Pasqualato, A. Romussi, F. Thaler, P. Trifiro, M. Villa, S. Vultaggio, O.A. Botrugno, P. Dessanti, S. Minucci, E. Zaggarri, D. Carettoni, L. Iuzzolino, M. Varasi, P. Vianello, Thieno[3,2-b]pyrrole-5-carboxamides as New Reversible Inhibitors of Histone Lysine Demethylase KDM1A/LSD1. Part 1: High-Throughput Screening and Preliminary Exploration, *J Med Chem* 60(5) (2017) 1673-1692.

[19] M.L. Schmitt, A.T. Hauser, L. Carlino, M. Pippel, J. Schulz-Fincke, E. Metzger, D. Willmann, T. Yiu, M. Barton, R. Schule, W. Sippl, M. Jung, Nonpeptidic propargylamines as inhibitors of lysine specific demethylase 1 (LSD1) with cellular activity, *J Med Chem* 56(18) (2013) 7334-7342.

[20] S.K. Sharma, Y. Wu, N. Steinbergs, M.L. Crowley, A.S. Hanson, R.A. Casero, P.M. Woster, (Bis)urea and (bis)thiourea inhibitors of lysine-specific demethylase 1 as epigenetic modulators, *J Med Chem* 53(14) (2010) 5197-5212.

[21] F. Wu, C. Zhou, Y. Yao, L. Wei, Z. Feng, L. Deng, Y. Song, 3-(Piperidin-4-ylmethoxy)pyridine Containing Compounds Are Potent Inhibitors of Lysine Specific Demethylase 1, *J Med Chem* 59(1) (2016) 253-263.

[22] C. Yang, W. Wang, J.X. Liang, G. Li, K. Vellaisamy, C.Y. Wong, D.L. Ma, C.H. Leung, A Rhodium(III)-Based Inhibitor of Lysine-Specific Histone Demethylase 1 as an Epigenetic Modulator in Prostate Cancer Cells, *J Med Chem* 60(6) (2017) 2597-2603.

[23] Y.C. Zheng, Y.C. Duan, J.L. Ma, R.M. Xu, X. Zi, W.L. Lv, M.M. Wang, X.W.

Ye, S. Zhu, D. Mobley, Y.Y. Zhu, J.W. Wang, J.F. Li, Z.R. Wang, W. Zhao, H.M. Liu, Triazole-dithiocarbamate based selective lysine specific demethylase 1 (LSD1) inactivators inhibit gastric cancer cell growth, invasion, and migration, *J Med Chem* 56(21) (2013) 8543-8560.

[24] N. Sugino, M. Kawahara, G. Tatsumi, A. Kanai, H. Matsui, R. Yamamoto, Y. Nagai, S. Fujii, Y. Shimazu, M. Hishizawa, T. Inaba, A. Andoh, T. Suzuki, A. Takaori-Kondo, A novel LSD1 inhibitor NCD38 ameliorates MDS-related leukemia with complex karyotype by attenuating leukemia programs via activating super-enhancers, *Leukemia* 31(11) (2017) 2303-2314.

[25] M.T. Borrello, B. Schinor, K. Bartels, H. Benelkebir, S. Pereira, W.T. Al-Jamal, L. Douglas, P.J. Duriez, G. Packham, G. Haufe, Fluorinated tranylcypromine analogues as inhibitors of lysine-specific demethylase 1 (LSD1, KDM1A), *Bioorg Med Chem Lett* 27(10) (2017) 2099-2101.

[26] T. Maes, C. Mascaro, I. Tirapu, A. Estiarte, F. Ciceri, S. Lunardi, N. Guibourt, A. Perdones, M.M.P. Lufino, T.C.P. Somerville, D.H. Wiseman, C. Duy, A. Melnick, C. Willekens, A. Ortega, M. Martinell, N. Valls, G. Kurz, M. Fyfe, J.C. Castro-Palomino, C. Buesa, ORY-1001, a Potent and Selective Covalent KDM1A Inhibitor, for the Treatment of Acute Leukemia, *Cancer cell* 33(3) (2018) 495-511.

[27] H.P. Mohammad, K.N. Smitheman, C.D. Kamat, D. Soong, K.E. Federowicz, G.S. Van Aller, J.L. Schneck, J.D. Carson, Y. Liu, M. Butticello, W.G. Bonnette, S.A. Gorman, Y. Degenhardt, Y. Bai, M.T. McCabe, M.B. Pappalardi, J. Kasparec, X. Tian, K.C. McNulty, M. Rouse, P. McDevitt, T. Ho, M. Crouthamel, T.K. Hart, N.O. Concha, C.F. McHugh, W.H. Miller, D. Dhanak, P.J. Tummino, C.L. Carpenter, N.W. Johnson, C.L. Hann, R.G. Kruger, A DNA Hypomethylation Signature Predicts Antitumor Activity of LSD1 Inhibitors in SCLC, *Cancer cell* 28(1) (2015) 57-69.

[28] D. Rotili, S. Tomassi, M. Conte, R. Benedetti, M. Tortorici, G. Ciossani, S. Valente, B. Marrocco, D. Labella, E. Novellino, A. Mattevi, L. Altucci, A. Tumber, C. Yapp, O.N.F. King, R.J. Hopkinson, A. Kawamura, C.J. Schofield, A. Mai, Pan-Histone Demethylase Inhibitors Simultaneously Targeting Jumonji C and Lysine-Specific

- Demethylases Display High Anticancer Activities, *J Med Chem* 57(1) (2013) 42-55.
- [29] J. Schulz-Fincke, M. Hau, J. Barth, D. Robaa, D. Willmann, A. Kurner, J. Haas, G. Greve, T. Haydn, S. Fulda, M. Lubbert, S. Ludeke, T. Berg, W. Sippl, R. Schule, M. Jung, Structure-activity studies on N-Substituted tranlycypromine derivatives lead to selective inhibitors of lysine specific demethylase 1 (LSD1) and potent inducers of leukemic cell differentiation, *Eur J Med Chem* 144 (2018) 52-67.
- [30] Y.C. Duan, Y.C. Ma, W.P. Qin, L.N. Ding, Y.C. Zheng, Y.L. Zhu, X.Y. Zhai, J. Yang, C.Y. Ma, Y.Y. Guan, Design and synthesis of tranlycypromine derivatives as novel LSD1/HDACs dual inhibitors for cancer treatment, *Eur J Med Chem* 140 (2017) 392-402.
- [31] M. Pieroni, G. Annunziato, E. Azzali, P. Dessanti, C. Mercurio, G. Meroni, P. Trifiro, P. Vianello, M. Villa, C. Beato, M. Varasi, G. Costantino, Further insights into the SAR of alpha-substituted cyclopropylamine derivatives as inhibitors of histone demethylase KDM1A, *Eur J Med Chem* 92 (2015) 377-386.
- [32] P.K. Chinthakindi, T. Naicker, N. Thota, T. Govender, H.G. Kruger, P.I. Arvidsson, Sulfonimidamides in Medicinal and Agricultural Chemistry, *Angew. Chem. Int. Ed.* 56(15) (2017) 4100-4109.
- [33] P. Vianello, O.A. Botrugno, A. Cappa, R. Dal Zuffo, P. Dessanti, A. Mai, B. Marrocco, A. Mattevi, G. Meroni, S. Minucci, G. Stazi, F. Thaler, P. Trifiro, S. Valente, M. Villa, M. Varasi, C. Mercurio, Discovery of a Novel Inhibitor of Histone Lysine-Specific Demethylase 1A (KDM1A/LSD1) as Orally Active Antitumor Agent, *J Med Chem* 59(4) (2016) 1501-1517.
- [34] Y. Ishikawa, K. Gamo, M. Yabuki, S. Takagi, K. Toyoshima, K. Nakayama, A. Nakayama, M. Morimoto, H. Miyashita, R. Dairiki, Y. Hikichi, N. Tomita, D. Tomita, S. Imamura, M. Iwatani, Y. Kamada, S. Matsumoto, R. Hara, T. Nomura, K. Tsuchida, K. Nakamura, A Novel LSD1 Inhibitor T-3775440 Disrupts GFI1B-Containing Complex Leading to Transdifferentiation and Impaired Growth of AML Cells, *Mol Cancer Ther* 16(2) (2017) 273-284.
- [35] E.H. Huntress, F.H. Carten, Identification of Organic Compounds. I.

Chlorosulfonic Acid as a Reagent for the Identification of Aryl Halides, *J Am Chem Soc* 62(3) (1940) 1715-1717.

[36] J.P. McGrath, K.E. Williamson, S. Balasubramanian, S. Odate, S. Arora, C. Hatton, T.M. Edwards, T. O'Brien, S. Magnuson, D. Stokoe, D.L. Daniels, B.M. Bryant, P. Trojer, Pharmacological Inhibition of the Histone Lysine Demethylase KDM1A Suppresses the Growth of Multiple Acute Myeloid Leukemia Subtypes, *Cancer research* 76(7) (2016) 1975-1988.

[37] K.N. Smitheman, T.M. Severson, S.R. Rajapurkar, M.T. McCabe, N. Karpnich, J. Foley, M.B. Pappalardi, A. Hughes, W. Halsey, E. Thomas, C. Traini, K.E. Federowicz, J. Laraio, F. Mobegi, G. Ferron-Brady, R.K. Prinjha, C.L. Carpenter, R.G. Kruger, L. Wessels, H.P. Mohammad, Lysine specific demethylase 1 inactivation enhances differentiation and promotes cytotoxic response when combined with all-trans retinoic acid in acute myeloid leukemia across subtypes, *Haematologica* 104(6) (2019) 1156-1167.

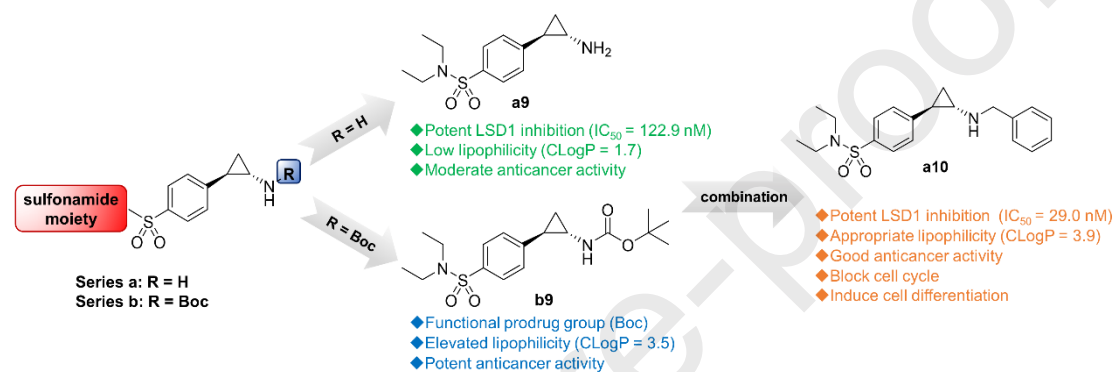
[38] W. Fiskus, S. Sharma, B. Shah, B.P. Portier, S.G. Devaraj, K. Liu, S.P. Iyer, D. Bearss, K.N. Bhalla, Highly effective combination of LSD1 (KDM1A) antagonist and pan-histone deacetylase inhibitor against human AML cells, *Leukemia* 28(11) (2014) 2155-2164.

[39] S. Wen, J. Wang, P. Liu, Y. Li, W. Lu, Y. Hu, J. Liu, Z. He, P. Huang, Novel combination of histone methylation modulators with therapeutic synergy against acute myeloid leukemia in vitro and in vivo, *Cancer letters* 413 (2018) 35-45.

Declaration of interests

The authors declare that they have no known competing financial interests or personal relationships that could have appeared to influence the work reported in this paper.

Graphical Abstract



Highlights

- 21 novel compounds with para-sulfonamides based on TCP scaffolding were synthesized to provide a potent LSD1 inhibitor with IC_{50} of 29 nM.
- Boc was found to be a potential prodrug functional group which enhanced cellular uptake of LSD1 inhibitors and improved their anti-proliferation activity.
- Appropriate lipophilicity and potent LSD1 inhibition contributed to the improved anti-proliferation effect towards acute myeloid leukemia of LSD1 inhibitors.